

# Flexural behavior of full-scale, carbon-fiber-reinforced polymer prestressed concrete beams

Prakash Poudel, Abdeldjelil Belarbi, Bora Gencturk, and Mina Dawood

- In the past few decades, carbon-fiber-reinforced polymers (CFRPs) have been researched and implemented in concrete structures to address problems related to environmental durability and increase the service lives of bridges. This paper addresses a gap in the research and application of CFRP prestressing elements in large-scale bridge beams.
- Eight full-scale American Association of State Highway and Transportation Officials (AASHTO) Type I prestressed concrete beams pretensioned with CFRP cables, CFRP bars, or steel prestressing strands were tested under monotonic and fatigue loading to evaluate the flexural behavior, load-deflection behavior, and ultimate capacity of the beams.
- The experimental results were compared with analytical predictions and indicated that the flexural behavior and capacity of the beams can be accurately predicted with analytical models. The results also show that the CFRP prestressed concrete beams exhibit enough cracking and deflection to provide advanced warning of potential failure.

**T**oday's highway bridge construction almost exclusively uses steel prestressing strands for prestressed concrete beams. Prestressing steel is susceptible to corrosion-induced degradation when exposed to aggressive environments. Corrosion can result in the deterioration of the serviceability and strength of highway bridge beams. These concerns have led to the use of nonmetallic prestressing elements made of glass-fiber-reinforced polymer (GFRP), aramid-fiber-reinforced polymer (AFRP), and carbon-fiber-reinforced polymer (CFRP) materials, which are collectively referred to as fiber-reinforced polymers (FRPs). Among FRPs, CFRP has the greatest potential to replace steel strands and provide corrosion-free prestressed concrete bridge girders when combined with corrosion-resistant transverse reinforcement. Completed examples of CFRP prestressed concrete beam implementations in the United States include the Pembroke Avenue Bridge and Plum Creek Bridge in Michigan. Examples in progress include the Interstate 64 South Side High Rise Bridge and Laskin Road Bridge in Virginia.<sup>1</sup> Although the initial cost of CFRP is higher than that of GFRP and AFRP, all three FRP types exhibit higher tensile strengths than prestressing steel, and CFRP stands out as a viable option because of its high modulus of elasticity and better creep performance. The durability properties of CFRP are also excellent compared with other FRPs. The strength reduction of FRP exposed to different environmental (alkaline, moisture, saline, and ultraviolet) and mechanical (fatigue and stress rupture) effects was found to be less than 23% for CFRP (ultraviolet), 55% for AFRP (stress rupture), and 28% for GFRP (alkaline

at 140°F [60°C]).<sup>2</sup> A recent study by Benmokrane et al.<sup>3</sup> on the durability performance of prestressing CFRP exposed to elevated temperature and an alkaline environment found that under extreme conditions (a 7000-hour immersion in an alkaline solution at 140°F), the reduction in tensile strength was only about 7%. This paper investigates the flexural behavior of American Association of State Highway and Transportation Officials (AASHTO) Type I CFRP prestressed concrete beams based on full-scale experimental results.

## Background and motivation

For the past two decades, prestressing concrete with CFRP has been an area of active research and this technology is developing through research studies and implementation projects in bridge beams and piles. An experimental database of concrete beams that were prestressed with prestressing CFRP was compiled to assess the state-of-the-art of experimental research on CFRP prestressed concrete beams and identify research gaps.<sup>4</sup> The database includes 264 beams that were independently reported in 41 publications from around the world. **Figure 1** summarizes the distribution of some of the key parameters in the experimental database that influence the flexural behavior of these beams. The figure shows that the previous experimental studies focused primarily on pretensioned beams. This is mainly because pretensioned beams are more common than their post-tensioned counterparts in highway bridges. Most of the tested beams (96%) had heights of less than 20 in. (508 mm). This is in contrast to the industry standard prestressed concrete bridge beams, where

20 in. is closer to the lower bound of what is typically used. In addition, most of the tested beams had a rectangular cross section with a span length less than 30 ft (9.1 m). I-beams with a composite cast-in-place concrete deck slab are most commonly used in bridge construction, with a trend toward using decked bulb-type girders. Small-diameter (less than 0.5 in. [12.7 mm]) CFRP cables and bars were used in the previous experimental studies, some of which are no longer in production. The experimental database sheds light on one of the gaps in the continuum of research on the flexural behavior of CFRP prestressed concrete beams: the lack of experimental data on large-scale composite prestressed concrete girders for bridge construction prestressed with 0.5 in. or larger diameter prestressing CFRP, which is representative of the current construction practice.

Small-scale specimens can be easily fabricated, are not costly, and can be tested without heavy moving, rigging, or testing equipment, allowing experimental testing of several parameters in the same study. However, the design and fabrication processes of small-scale beams do not always use conventional materials, industry standards, and equipment. As such, although small-scale beams are useful for investigating a larger number of design variables, large- or full-scale testing is necessary to understand the material and system performance issues that may be encountered in real practice. Some of the features of CFRP prestressed concrete beams that cannot be effectively captured in small-scale testing include aggregate size, anchorage placement, coupler positioning, and coupling of CFRP with steel prestressing strands.

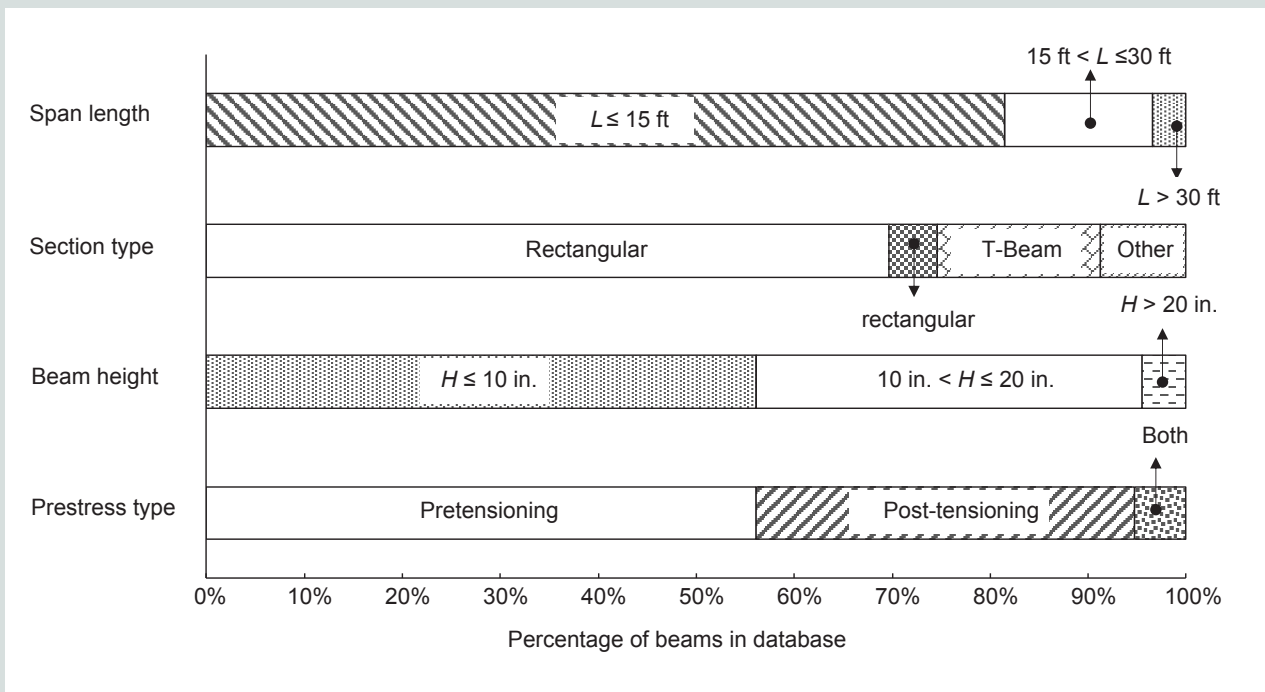


**Figure 1.** Distribution of key parameters from previous experimental studies. Note:  $H$  = height of beam;  $L$  = span length. 1 in. = 25.4 mm; 1 ft = 0.305 m.

Because of the linear elastic nature of prestressing CFRP up to failure, there are two possible failure modes for CFRP prestressed concrete beams: tension controlled (rupture of prestressing CFRP) and compression controlled (concrete crushing). Previous experimental studies consistently demonstrated that the deformation at ultimate load is less for beams pretensioned with prestressing CFRP than for beams prestressed with steel prestressing strands if both beams are designed as tension controlled (failure by rupture of the prestressing reinforcement). The lower deformation can be attributed to the low rupture strain of CFRP compared with that of steel (about 2% for prestressing CFRP compared with about 6% for prestressing steel). The brittle failure and the lower deformation of CFRP prestressed concrete beams because of inherent CFRP material properties are a concern in design; however, if both steel and CFRP prestressed concrete beams are designed to fail by crushing of concrete (compression-controlled), the deformation at ultimate load was found to be very similar.<sup>5</sup>

Nearly all highway bridge beams are designed with a composite concrete deck, and compression-controlled design (crushing of concrete) of CFRP prestressed concrete beams with a composite deck poses several challenges. First, a large amount of prestressing reinforcement would be required to induce such failure, which would increase the cost of the beams. Second, the concrete section size would have to be reduced, creating an unrealistic (nonstandard) highway section.<sup>6</sup> This is because when a deep section is used, the strain in the prestressing CFRP exceeds the rupture strain before the concrete reaches its ultimate compressive strain. Therefore, the section depth must be reduced until a compressive failure is achieved before rupture of the prestressing CFRP. However, one advantage of designing CFRP prestressed concrete beams for concrete crushing failure is the improved deformability of CFRP prestressed concrete beams using partial prestressing and using both bonded and unbonded prestressing CFRP.<sup>7,8</sup> In addition, the vertical arrangement of prestressed and nonprestressed CFRP was found to induce progressive failure and thus increase the deformability of the CFRP prestressed concrete beams failing due to the rupture of prestressing CFRP.<sup>9</sup> Grace and Singh<sup>8</sup> recommended that beams be designed for concrete crushing failure because of the higher deformability achieved compared with prestressing CFRP rupture. However, all of these conclusions regarding the deformability of the beams rely on energy-based models that are insensitive to the magnitude of the ultimate deformation of the member.<sup>10,11</sup> This may be appropriate for applications where energy absorption is a primary design consideration (for example, seismic design); however for bridge beams, deformation before failure is a more important consideration than energy dissipation. As such, a definition of deformability that is based on deformation before failure may be more suitable. Studies have shown that the inclusion of distinct deformation parameters, such as ultimate and cracking deformations, in the deformability index provides a reasonable measure of the performance of CFRP prestressed concrete beams.<sup>5,12</sup>

This paper investigates the flexural behavior of tension-controlled (failure due to CFRP rupture) AASHTO Type I CFRP prestressed concrete beams with composite action from a reinforced concrete deck based on full-scale experimental results. The tension-controlled failure is the most realistic design for CFRP prestressed concrete beams, and it is the most commonly used design approach.<sup>4</sup> The flexural behavior is discussed in terms of load-deflection and load-strain responses as well as failure modes. In addition, the flexural behavior of CFRP prestressed concrete beams is compared with an identically designed prestressed concrete beam using steel prestressing strands. This paper also discusses the additional requirements for the construction of CFRP prestressed concrete beams if a practice similar to that of prestressed concrete beams using steel prestressing strands is followed. Current formulations to predict the nominal strength of CFRP prestressed concrete beams are also evaluated against the experimental data. In addition to providing valuable experimental data on full-scale beams, the evaluation of existing formulations and the additional requirements in CFRP prestressed concrete beam construction provided in this paper are expected to advance the current research on this topic.

## Experimental program

The experimental program included the design, construction, testing, and analysis of seven full-scale CFRP prestressed concrete beams (three beams with CFRP cables and four with CFRP bars) and one prestressed concrete beam using steel prestressing strands. The test beams were AASHTO Type I with a 39.5 ft (12.0 m) span length and an 8 in. (200 mm) thick composite concrete deck. Two flexural loading conditions were considered: monotonic flexure and flexural fatigue. **Table 1** shows the test matrix for the experimental program. The two CFRP prestressed concrete beams that were tested under flexural fatigue were subjected to 2.3 million cycles.

**Table 1.** Test matrix

Type of prestressing	Type of loading	Number of repetitions	Beam identification
CFRP cable (Ca)	Monotonic (M)	2	Ca_B_M#
	Flexural fatigue (F)	1	Ca_B_F
CFRP bar (Ba)	Monotonic (M)	2	Ba_B_M#
	Flexural fatigue (F)	1	Ba_B_F
	Monotonic (M)	1	Ba_Pd_M
Steel strands (St)	Monotonic (M)	1	St_B_M

Note: CFRP = carbon-fiber-reinforced polymer.

The beam identification presented in Table 1 includes the following information in this order:

1. prestressing CFRP type (CFRP cable labeled Ca, CFRP bar labeled Ba, or steel cable labeled St)
2. type of loading (static monotonic loading labeled M or cyclic fatigue loading labeled F)
3. the repetition number if more than one test was conducted
4. bond designation (fully bonded labeled B or partially debonded labeled Pd)

For example, Ca\_B\_M#1 is a beam prestressed with CFRP cables (Ca), fully bonded (B), and subjected to static monotonic loading (M), and it is the first repetition of two identical tests. The two identical monotonic loading specimens were fabricated to ensure the repeatability of the ultimate capacity using the same construction and testing procedures. Six beams (one with prestressing steel and five with prestressing CFRP) were tested monotonically to failure without any prior fatigue loading. All of the prestressed concrete beams were fabricated at a precast concrete facility and transported to the structural laboratory at the University of Houston for testing.

## Materials

Two types of prestressing CFRP reinforcement were used: 0.5 in. (12.7 mm) diameter CFRP bars with solid circular cross sections and 0.6 in. (15.2 mm) diameter CFRP cables, which consist of seven individual wires twisted together into a

single strand similar to a steel prestressing strand. In addition to the CFRP reinforcement, one beam was prestressed with 0.6 in. diameter steel strands (**Table 2**).

A tension test was performed according to ASTM D7205<sup>13</sup> on the prestressing CFRP used in the experimental program to characterize the guaranteed and ultimate (or rupture) load and strain. Ten specimens with a length of 60 in. (1520 mm) were prepared from the batch of prestressing CFRP used in the beams. A potted-type anchorage system that consists of a highly expansive material enclosing the prestressing CFRP inside a steel tube was used at the gripping locations. **Figure 2** shows the schematic of the specimen with the anchorage lengths for both the CFRP cable and the bar. Each specimen was instrumented with one strain gauge with a strain limit of 5% and an extensometer with a gauge length of 2 in. (50 mm) to measure elongation. A loading frame with a tensile loading capacity of 110 kip (490 kN) was used for testing. Applied load and corresponding specimen elongation were recorded using a data acquisition system. The applied load was also recorded using the built-in data acquisition system of the test frame. Besides the tensile strength and tensile strain, the modulus of elasticity of the prestressing CFRP was calculated based on the measured data according to ASTM D7205.<sup>13</sup> Table 2 presents the material properties of the reinforcement obtained from these tests.

The concrete had a design 28-day compressive strength of 4 ksi (28 MPa) for the deck and 9 ksi (62 MPa) for the beams. All beams were fabricated using self-consolidating concrete. During each casting, 16 standard-size cylinders (4 × 8 in. [100 × 200 mm]) were cast to determine the concrete strength

**Table 2.** Properties of prestressing material used

Prestressing material type	Guaranteed load, kip	Rupture load, kip	Modulus of elasticity, ksi	Rupture strain, %
CFRP cable	66.8	73.7	21,670	1.9
CFRP bar	50.9	54.9	20,630	1.3
Steel strands	52.7*	58.0	29,000	1.00†

Note: CFRP = carbon-fiber-reinforced polymer. 1 kip = 4.448 kN; 1 ksi = 6.895 MPa.

\* Yield strength.

† Yield strain.

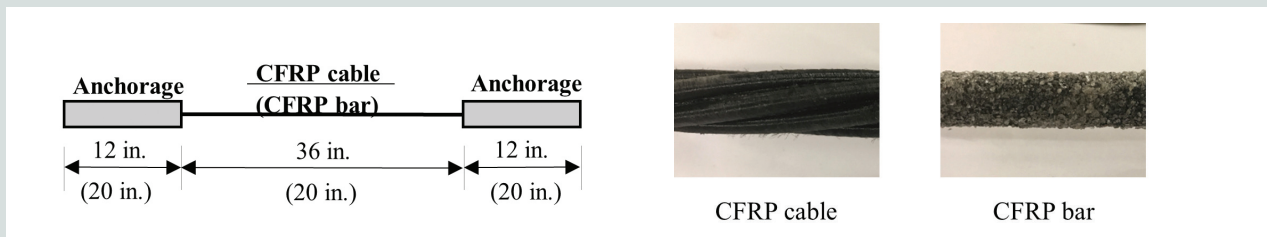


**Figure 2.** Schematic of tensile test specimens with anchorages: carbon-fiber-reinforced polymer cable and carbon-fiber-reinforced polymer bars. Note: CFRP = carbon-fiber-reinforced polymer. 1 in. = 25.4 mm.

according to ASTM C39/C39M.<sup>14</sup> The cylinders were kept in cylinder molds in the same environmental conditions as the beams until the day of testing. The average concrete strengths for the beam and the deck were 10.7 and 9.1 ksi (73.8 and 62.7 MPa), respectively, for the CFRP prestressed concrete beams. The average concrete strengths for the beam and the deck were 11.2 and 4.2 ksi (77.2 and 29.0 MPa), respectively, for the prestressed beam using steel strands.

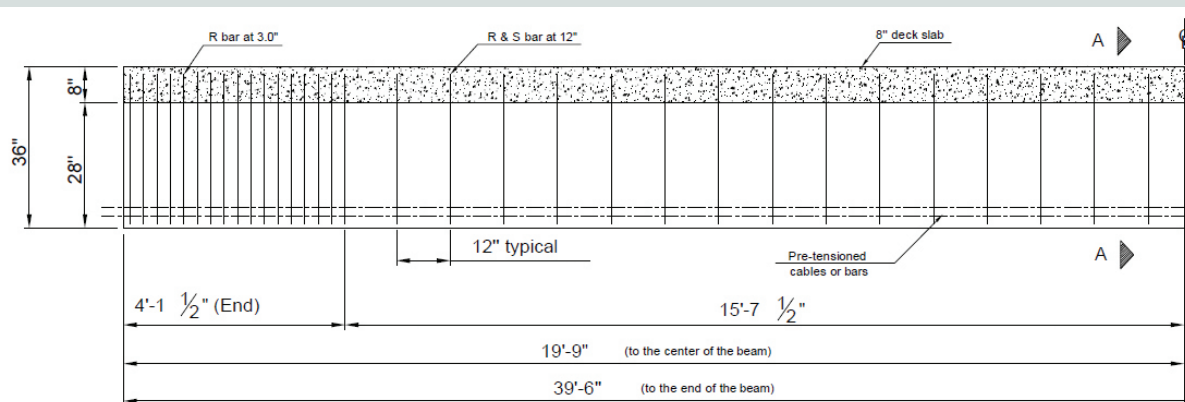
## Beam design

Figure 3 shows the geometry and reinforcement detailing of all CFRP prestressed concrete beams. The prestressing CFRP was tensioned to 60% of the design strength such that 40% reserve strain was available for flexure. The steel prestressing strands were tensioned to 70% of the ultimate tensile load. All test beams were designed to fail due to the rupture of the prestressing elements. The number of prestressing CFRP cables was selected such that the area of the provided CFRP (1.73 in.<sup>2</sup> [1120 mm<sup>2</sup>], eight CFRP cables) was close to the balanced reinforcement area (1.70 in.<sup>2</sup> [1100 mm<sup>2</sup>] based on the guaranteed tensile strength) of a noncomposite

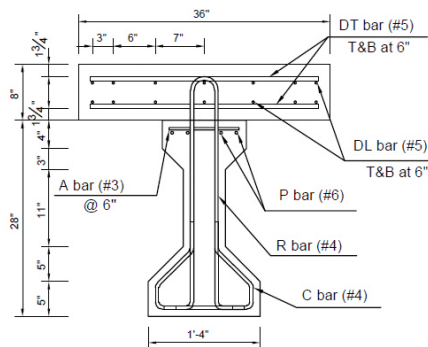
AASHTO Type I beam. After the composite deck was added to the beam, CFRP rupture failure mode controls as the area of the CFRP provided becomes 25% of the balanced reinforcement area of the composite beam. The area of CFRP provided becomes 49% of the balanced reinforcement area if the rupture strength of CFRP is used in the calculation. Furthermore, to facilitate a direct comparison, the prestressed concrete beam with steel prestressing strands was constructed with eight steel strands (with the same diameter as the CFRP cable). For the beams prestressed with prestressing CFRP bars, the number of bars (12 CFRP bars) was selected so that the total load at ultimate is similar to that of the beam prestressed with CFRP cables. The detailing and design of anchorage zone and shear reinforcement were performed according to the *AASHTO LRFD Bridge Design Specifications*<sup>15</sup> for beams prestressed with both CFRP and steel.

## Fabrication of test beams

All pretensioned beams were fabricated at a precasting facility. The prestressing CFRP bars came in fixed lengths from the manufacturer, hence each of the beams pretensioned with



Elevation view of the beam with shear reinforcement



Section A-A

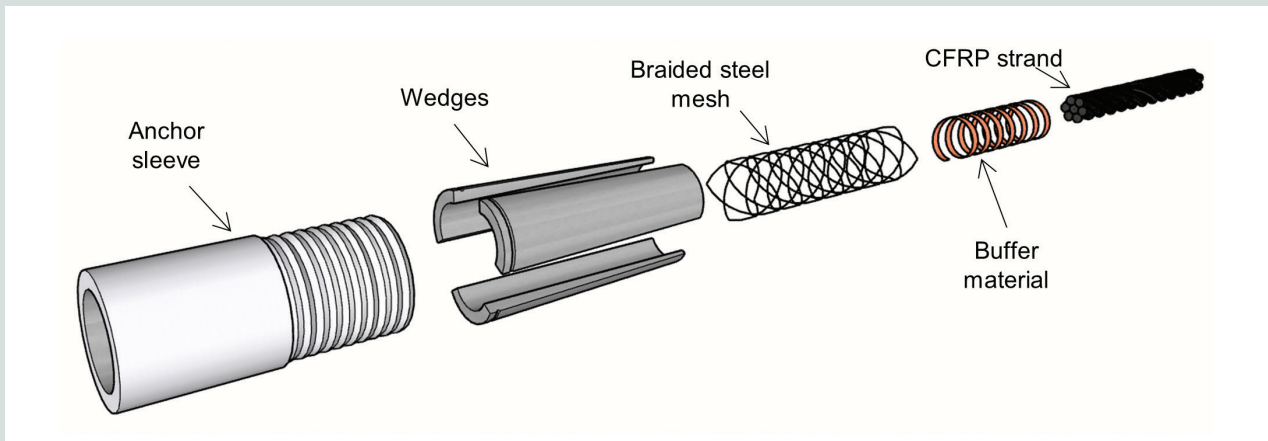
Cross-sectional view

Figure 3. Elevation view and cross-sectional details of full-scale prestressed concrete beams. Note: CL = centerline; DL = deck longitudinal reinforcement; DT = deck transverse reinforcement; T&B = top and bottom. 1" = 1 in. = 25.4 mm; 1' = 1 ft = 0.3 m.

CFRP bars had to be placed separately. The CFRP cables were received in a spool from the manufacturer, so it was possible to cut the cables to the desired lengths and fabricate two beams at a time on the same prestressing bed. After the cables were cut to the required length for each beam, the anchorages were installed on the prestressing CFRP. The relatively low lateral and shear strength of CFRP prevents the use of conventional anchoring devices used for prestressing steel.<sup>16,17</sup> Therefore, special wedge anchors were installed on the CFRP cables and bars (Fig. 4 and 5). The anchors for both the CFRP cables and bars consisted of wedges, a sleeve, and a protective cover, such as a braided fabric with steel mesh or a copper sleeve surrounding the prestressing CFRP, to prevent localized damage from gripping. After the anchorages were placed for both cables and bars, the wedges were pushed inside the sleeves using a hydraulic device up to a pressure specified by the manufacturer.

The brittleness of the prestressing CFRP, as well as its low transverse strength, restricts the direct application of tension

through the CFRP anchorage during pretensioning. Therefore, the prestressing CFRP cables and bars were connected to the prestressing steel through a coupling fixture, also known as a coupler or transfer box. The couplers of the prestressing CFRP were connected to those of prestressing steel just outside the beam ends in a staggered manner to create the space needed for the larger transfer boxes. The prestressing CFRP and the steel strands with their respective anchorage system were positioned inside the transfer box such that when the steel strands are tensioned, the tension is directly transferred to the CFRP with no significant twist of the transfer box. After the prestressing CFRP cables or bars were tensioned, the transverse reinforcement for the girder was fixed in place. The transverse reinforcement extended 3 in. (75 mm) above the top face of the girder to create composite action with the deck slab. Then the forms were positioned and the self-consolidating concrete was placed inside the formwork. After the concrete cylinders, placed together with the beams, attained the target transfer strength of 5 ksi (34 MPa), the pre-



**Figure 4.** Anchorage for CFRP prestressing cable. Note: CFRP = carbon-fiber-reinforced polymer.

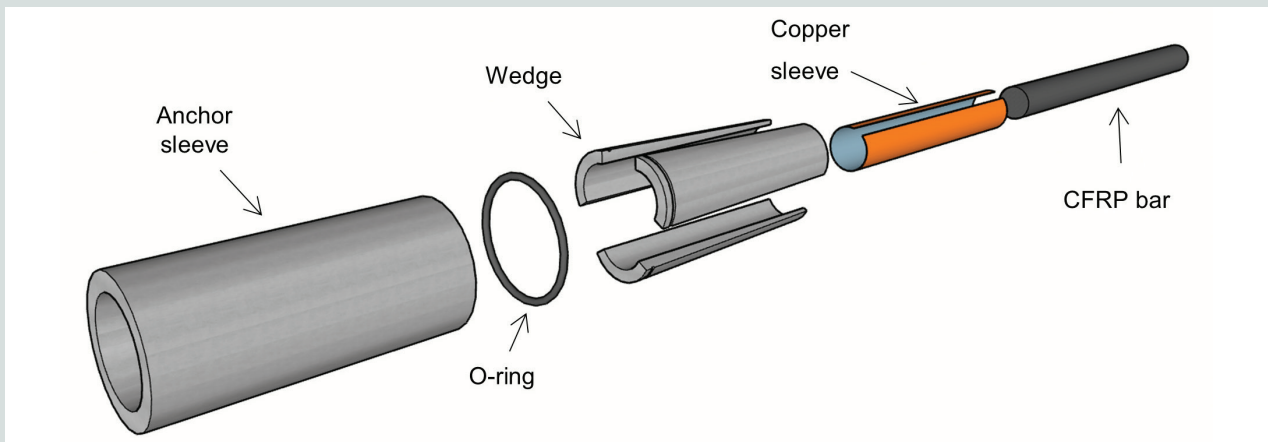


**Figure 5.** Anchorage for CFRP prestressing bars. Note: CFRP = carbon-fiber-reinforced polymer.

stressing force was transferred to the concrete by torch cutting the steel strands. Then forms for the composite deck were attached and the deck reinforcement was positioned inside the deck forms. Concrete was then placed inside the deck form to cast the composite deck. **Figure 6** shows the overall arrangement of the prestressing operation.

### Test setup, instrumentation, and loading protocol

The beams for both monotonic flexure and flexural fatigue were tested under four-point loading in simply supported conditions using a 235 kip (1045 kN) servo-hydraulic actuator and a spreader beam (**Fig. 7**). The load cells positioned at the supports had a 200 kip (890 kN) capacity. String potentiometers were positioned along the length of the beam (**Fig. 7**). The string potentiometers in the loading region had a 20 in. (510 mm) measurement range, and the remaining string potentiometers had a 7 in. (180 mm) measurement range. Each prestressing CFRP cable or bar was instrumented with two strain gauges, one at the midspan and one at the quarter span, with a strain limit of 5%. All of the instruments were monitored and recorded using a data acquisition system at a sampling rate of one sample per second.

For monotonic loading, a seating load was applied to the beam to eliminate the initial slack of the load application system and to seat the beam on its supports. The beams were tested in displacement control at a rate of 0.033 in./min (0.84 mm/min). After the first cracking point, the loading rate was increased to 0.167 in./min (4.24 mm/min) until 75% of the expected beam capacity was reached. Then the rate was decreased to 0.120 in./min (3.05 mm/min) until failure.

For the fatigue testing of CFRP prestressed concrete beams, the beam was initially loaded monotonically until the appearance of the fourth crack inside the constant moment region to simulate an accidental overload (**Fig. 8**). The load was then removed, and the beam was allowed to return to its original position. The beam was then loaded to the upper limit of the fatigue loading range, 72 kip (320 kN), which induces  $6\sqrt{f'_c}$  psi tensile stress in the outermost tension fiber of the CFRP prestressed concrete beam when the gross moment of inertia is used in the stress calculation and where  $f'_c$  is the concrete compressive strength. This upper limit of fatigue loading was chosen to correspond to the tensile limit of the extreme concrete fiber in service loading conditions based on the AASHTO LRFD specifications.<sup>14</sup> The lower limit of the fatigue loading range was 20 kip (90 kN), which was comput-

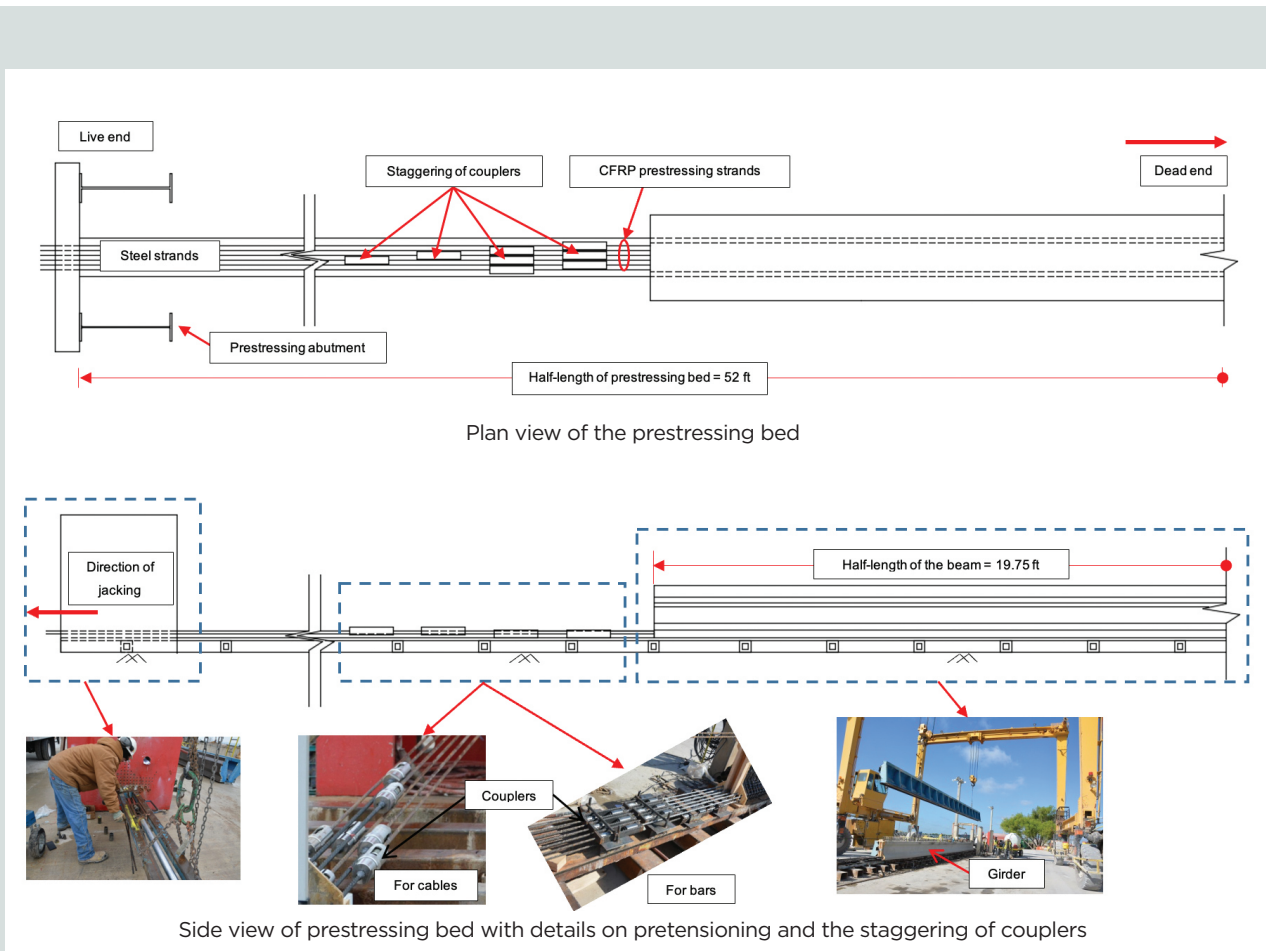


**Figure 6.** Overview of the prestressing bed and the staggering of CFRP couplers. Note: CFRP = carbon-fiber-reinforced polymer. 1 ft = 0.305 m.

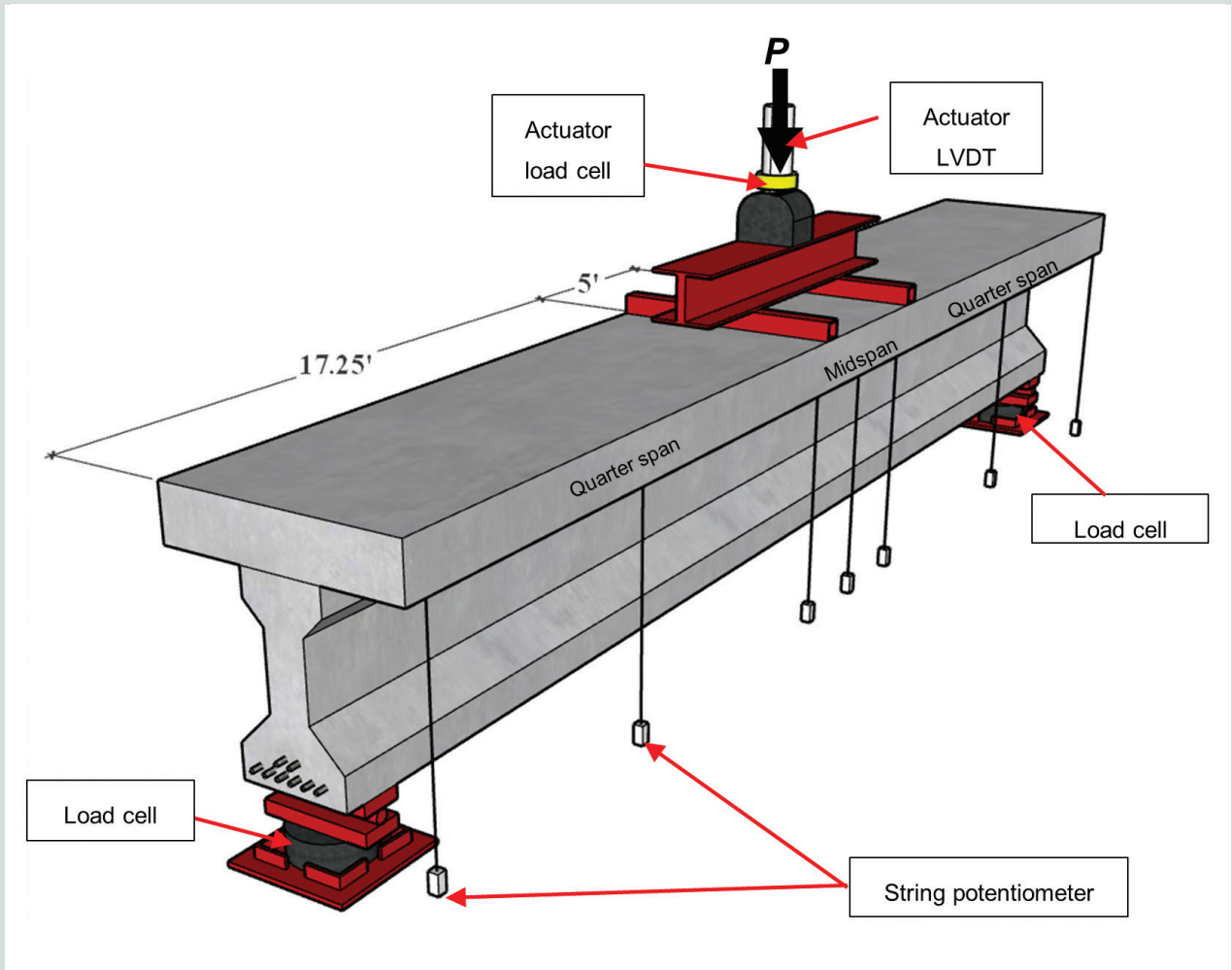


**Figure 7.** Test setup for flexure tests. Note: LVDT = linear variable displacement transducer;  $P$  = applied load. 1' = 1 ft = 0.305 m.

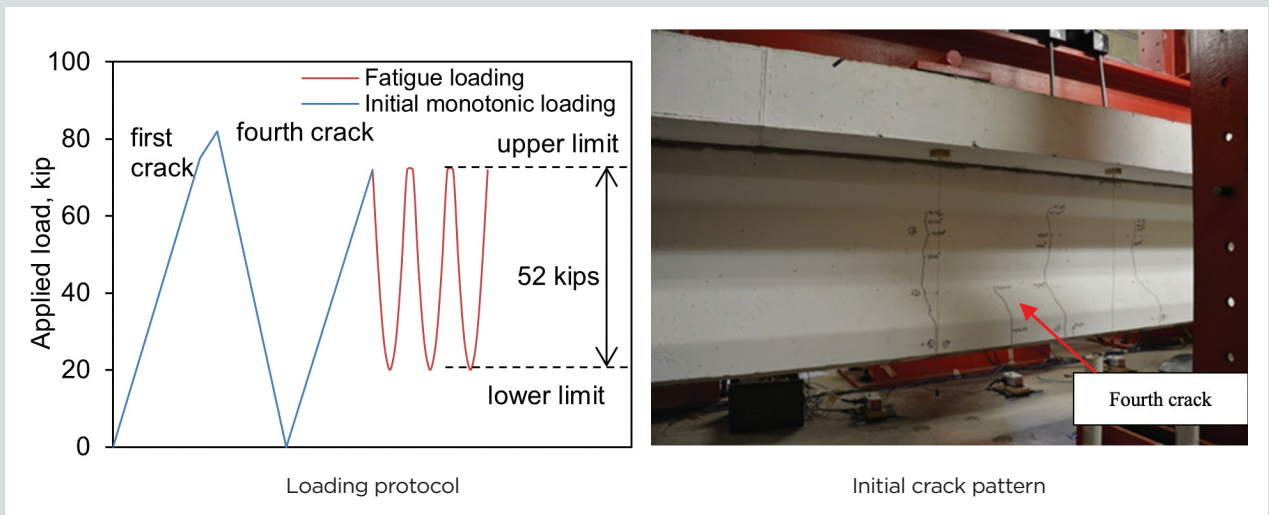


**Figure 8.** Flexural fatigue testing of carbon-fiber-reinforced polymer prestressed concrete beams. Note: 1 kip = 4.448 kN.



ed by subtracting the AASHTO fatigue truck moment from the value of the upper limit of the fatigue loading. The girder distribution factor was taken to be 1, which means that the entire fatigue load is assumed to be resisted by the test beam. The fatigue loading was applied at a frequency of 1 Hz. Every 500,000 cycles, the test was stopped and the beam was loaded monotonically to the upper limit of fatigue loading. The applied load, vertical deflections, prestressing CFRP strains, and crack widths were measured. A total of 2.3 million fatigue cycles were applied to the beams before monotonically loading to failure.

## Experimental results and discussion

### Prestressing force

The average initial prestressing forces (of all cables and bars per beam before transfer) measured from the strain gauges and load cells were 37.6, 28.5, and 40 kip (167, 127, and 178 kN), respectively, for beams prestressed with prestressing CFRP cables, prestressing CFRP bars, and prestressing steel. This corresponds to 62% and 57% of the guaranteed load for prestressing CFRP cables and bars, respectively. For prestressing steel, this load corresponds to 75% of the ultimate tensile strength. An average loss of 6% was observed due to elastic shortening of the beams prestressed with prestressing CFRP cables; for bars, the average loss was 8%. In addition,

up to the day of testing (average of 129 days), the beams prestressed with prestressing CFRP cables, prestressing CFRP bars, and prestressing steel experienced total losses of 13%, 22%, and 19%, respectively, in the initial prestressing force. The prestressing CFRP bars exhibited larger prestressing losses than the CFRP cables and steel strands.

### Camber

The camber measurements of all full-scale beams were taken after placing the decks and before testing. The average final camber (after placement of the composite deck) was 0.43 in. (11 mm) for the three beams prestressed with CFRP cables and 0.63 in. (16 mm) for the four beams prestressed with CFRP bars. The calculated final average camber (elastic) was 0.50 in. (13 mm) for the beams prestressed with CFRP cables and 0.60 in. (15 mm) for those prestressed with CFRP bars.

### Load-deflection behavior

The load-deflection behavior of the CFRP prestressed concrete beams was observed to be piece-wise linear with two distinct stiffnesses up to failure (Fig. 9). This behavior can be described using two distinct points as shown in the figure: the cracking point and the ultimate capacity. The initial stiffness of the beam decreased after the first cracking point and remained almost constant up to failure. The failure of the beam

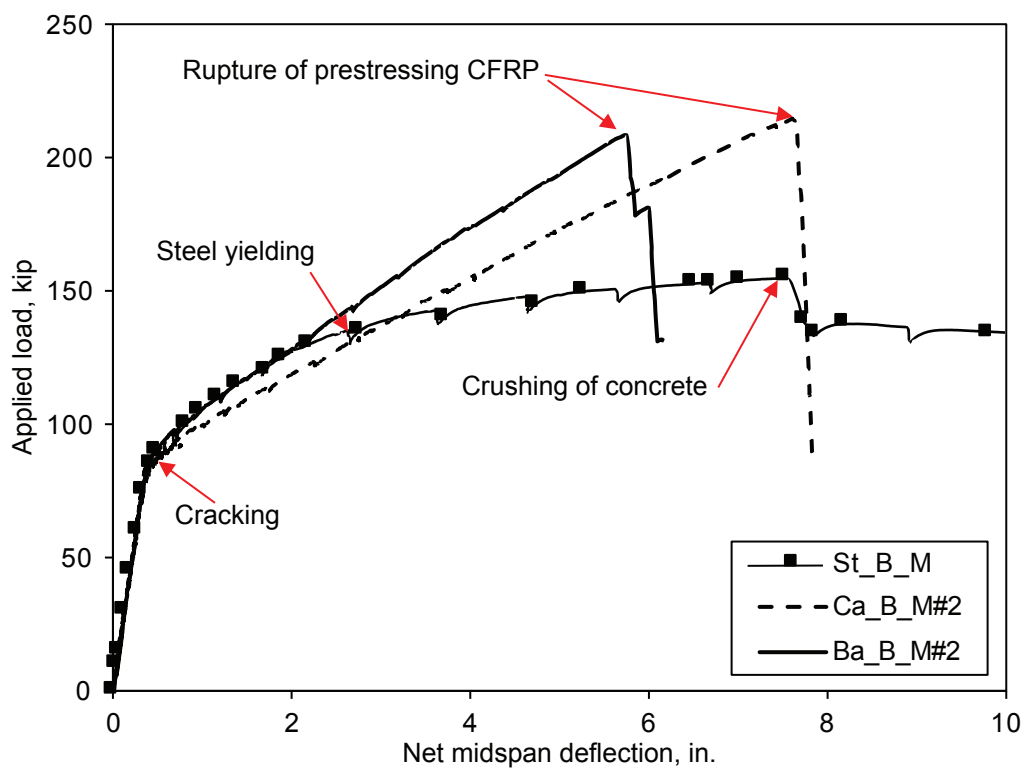


**Figure 9.** Load-deflection behavior of full-scale pretensioned concrete beams with CFRP or steel prestressing. Note: CFRP = carbon-fiber-reinforced polymer. 1 in. = 25.4 mm; 1 kip = 4.448 kN.

initiated when one of the prestressing CFRP cables on the bottom layer ruptured.

Figure 9 compares the load-deflection behavior of the beams with prestressing CFRP (Ca\_B\_M#2 and Ba\_B\_M#2) and prestressing steel (St\_B\_M). All beams exhibited a linear response up to cracking. In addition, the replacement of the prestressing steel with prestressing CFRP had a negligible impact on the uncracked stiffness and cracking load. This is expected because the beam geometry, total prestressing force, and eccentricity of the prestressing force were comparable. After cracking, the beam with prestressing CFRP cable had 20% lower stiffness than the beam with prestressing steel. This is due to the lower modulus of elasticity of the prestressing CFRP compared with the prestressing steel; however, the beam with prestressing CFRP bar exhibited similar stiffness to that of the beam with prestressing steel. This is because the number of prestressing CFRP bars used in the beams was greater than the number of CFRP cables, and although the modulus of elasticity of the CFRP bar used in this research was lower than that of steel, it was higher than that of the prestressing CFRP cable. The beam with prestressing steel exhibited a flat loading region after yielding of the prestressing steel. Beams prestressed with CFRP did not exhibit this behavior. Instead, the load continued to increase and the secondary stiffness of the beams remained constant. After yielding, the prestressed concrete beam with steel prestressing strands continued to deflect until failure ultimately occurred due to the crushing of the concrete followed by rupture of the prestressing steel. In contrast, the capacity of the beams prestressed with CFRP continued to increase until failure occurred due to rupture of the prestressing CFRP before crushing of the concrete. The flexural capacity of the CFRP prestressed concrete beams was nearly 1.5 times that of the prestressed concrete beam that used steel prestressing strands. The deflection of the beam when the CFRP cable ruptured was similar to that of the beam prestressed with prestressing steel when the concrete crushed; however, the deflection of the beam at the CFRP bar rupture was 27% lower than that of the beams with CFRP cable or prestressing steel. This can be

attributed to the difference in the reserve strain (the difference between the rupture strain and the effective prestressing strain) between the prestressing CFRP cable (0.011 in./in. [0.280 mm/mm]) and bar (0.005 in./in. [0.127 mm/mm]) because the CFRP bar has a lower rupture strain (1.3%) than that of the CFRP cable (1.9%) (Table 2). For steel prestressed concrete beams, this reserve strain is usually three to four times higher than that of CFRP prestressed concrete beams. Because the steel prestressed concrete beam failed due to the crushing of concrete, the reserve strain was not fully used.

**Table 3** presents a summary of the experimental data for the monotonic testing of full-scale CFRP prestressed concrete beams. The ultimate load and deflection and the cracking load are presented. The table shows that the CFRP prestressed concrete beams tested under monotonic loading failed at comparable loads. As designed, the combined tensile capacity of the prestressing reinforcement (the number of cables multiplied by the rupture load of one cable) was similar regardless of the prestressing CFRP type used; however, there were differences in the cracking load and the deflection of the beams. The difference in the cracking load was due to the initial prestress (14% higher for beams prestressed with CFRP bars) and the concrete strength of the girder on the day of testing. The difference in the deflection was because of the reserve strain in the prestressing CFRP after the initial prestressing as previously explained.

**Figure 10** shows the effect of fatigue loading on the stiffness of the two CFRP prestressed concrete beams during the fatigue cycles. The figure shows that the fatigue loading had an insignificant effect (less than 5%) on the stiffness of the CFRP prestressed concrete beams. After completion of the fatigue test, both beams were subjected to static monotonic loading up to failure. Figure 10 also shows the ultimate capacities obtained from the final monotonic tests of the fatigued beams along with the corresponding capacity of the beams tested under monotonic loading only. After 2.3 million cycles, the ultimate strength of the beams initially subjected to fatigue loading (Ca\_B\_F and Ba\_B\_F) was within 3% of those tested under monotonic loading only.

**Table 3.** Summary of the monotonic test results for full-scale beam testing

Beam identification	Cracking load, kip	Ultimate load, kip	Deflection at ultimate load, in.	Failure mode
Ca_B_M#1	75	206	8.0	Carbon-fiber-reinforced polymer rupture
Ca_B_M#2	88	214	7.6	
Ba_B_M#1	76	207	6.0	
Ba_B_M#2	86	209	5.8	
Ba_Pd_M	85	209	5.2	
St_B_M	84	155	7.8	Concrete crushing

Note: 1 in. = 25.4 mm; 1 kip = 4.448 kN.

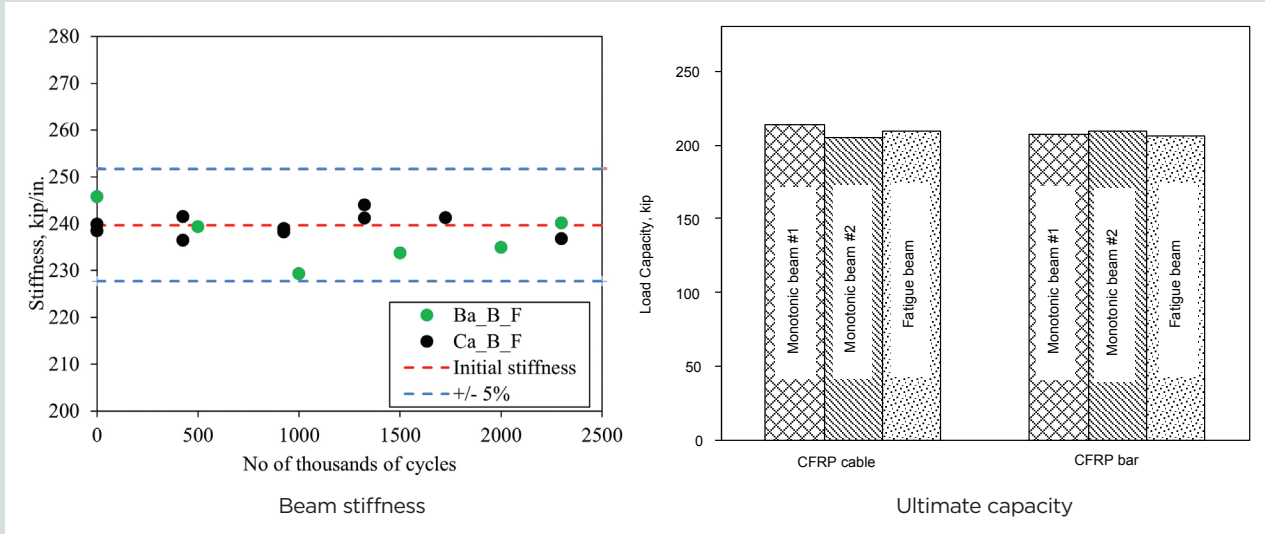


**Figure 10.** Effect of fatigue loading on beam stiffness and ultimate capacity. Note: 1 in. = 25.4 mm; 1 kip = 4.448 kN.

### Load-strain response

As previously mentioned, each cable in the test beams was instrumented with one strain gauge at the midspan of the beam. **Figure 11** shows the load-strain response of beam Ca\_B\_M#1. The strain gauges attached to the cable stopped recording at a load of 160 kip (710 kN). Hence, the curve was linearly extrapolated to determine the strain at failure. The extrapolated rupture strain at failure of the beam was 19,795  $\mu\epsilon$ , which is within 5% of the rupture strain of the prestressing CFRP cable, 19,000  $\mu\epsilon$  (Table 2). Similarly, the extrapolated

rupture strain for beam Ca\_B\_M#2 was 20,500  $\mu\epsilon$ , which is within 8% of the rupture strain obtained from material testing.

Figure 11 also shows the load-strain response of beam Ba\_B\_M#1. The rupture strain at the time of failure was 12,300  $\mu\epsilon$ , which is 5% lower than the rupture strain given in Table 2: 13,000  $\mu\epsilon$ . Similarly, the rupture strain in beam Ba\_B\_M#2 was 11,800  $\mu\epsilon$ , which is 9% lower than the rupture strain obtained from material testing. These results demonstrate that these beams were flexurally dominated and enabled an analysis using sectional properties as presented later in this paper.

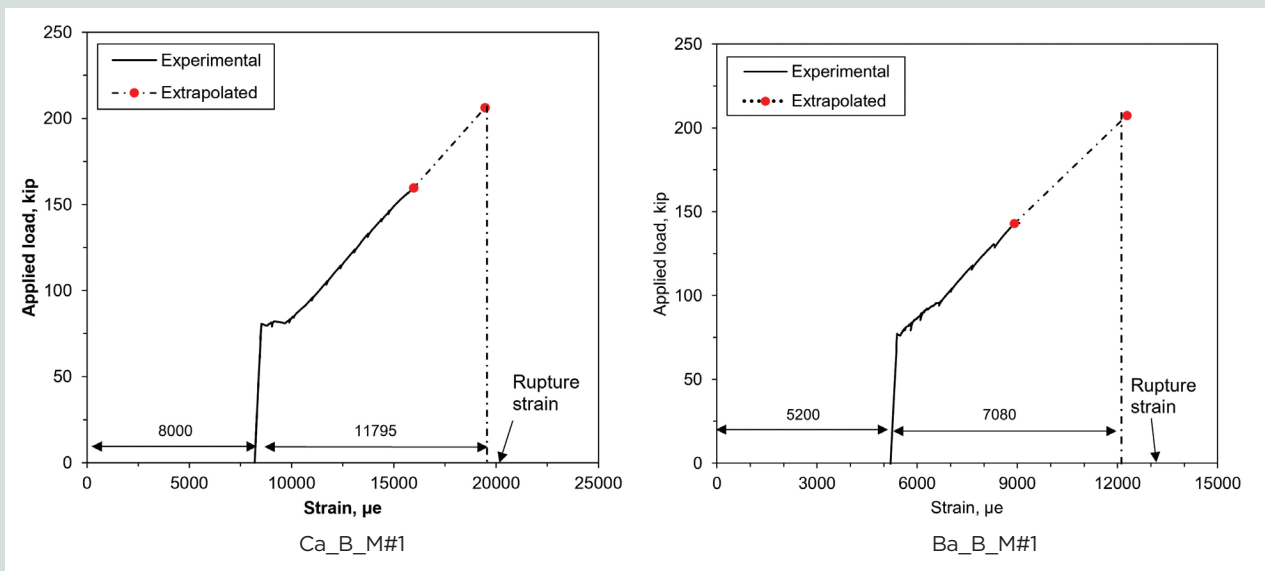


**Figure 11.** Load-strain response of carbon-fiber-reinforced polymer prestressed concrete beams. Note: 1 kip = 4.448 kN.

## Failure modes, crack distributions, and crack widths

For all CFRP prestressed concrete beams, failure was due to rupture of the prestressing CFRP; however, the steel prestressed concrete beams failed due to crushing of concrete. **Figure 12** shows the cracking pattern in each beam. As expected, the first crack on all prestressed concrete beams appeared inside the constant moment region. As the load increased, more cracks began to appear and the existing cracks widened. The width of the cracks was measured in stages up to twice the cracking load and at the final stage. For all beams, the cracks were spread over more than a quarter of the length from the center of the beam on each side (Fig. 12). At the ultimate failure, the CFRP prestressed concrete beams exhibited smaller crack widths and tighter crack spacing than the steel prestressed concrete beam. Figure 12 shows the maximum crack widths measured (at failure load) near the soffit of the CFRP prestressed concrete beams. The figure indicates that the crack widths of the beams prestressed with prestressing CFRP cables is 1.3 to 1.7 times that of the beams prestressed with CFRP bars. This is attributed to the higher longitudinal elastic modulus of the prestressing CFRP bars. In addition, the figure indicates that the beams with higher initial prestressing forces exhibit smaller crack widths. Beam Ca\_B\_M#2 had a higher initial prestressing force than both Ca\_B\_M#1 and Ca\_B\_F. Similarly, beam Ba\_B\_M#2 had a higher initial prestressing force than both Ba\_B\_M#1 and Ba\_B\_F.

## Analysis of test beams

### Analytical prediction of load-deflection response

The linear elastic behavior of the prestressing CFRP allows easy application of the strain-compatibility analysis to CFRP prestressed concrete beams to predict the ultimate strength. The analytical prediction of the test beams was carried out using software that performs the strain-compatibility analysis with a layer-by-layer approach.<sup>17</sup> The results from the software were verified with hand calculations. Before cracking, the capacity, as well as the deflection, can be accurately predicted using an elastic analysis; however, the behavior becomes complex after cracking in the CFRP prestressed concrete beams. One of the conventional ways to include the effect of tension stiffening is the use of an effective moment of inertia  $I_e$  in the elastic deflection equation instead of a gross moment of inertia  $I_g$ . ACI 440.4R-04<sup>19</sup> adopts the original equation by Branson,<sup>20</sup> which includes a softening factor to account for the lower modulus of elasticity of the CFRP to compute the effective moment of inertia as follows:

$$I_e = \left( \frac{M_{cr}}{M_a} \right)^3 \beta_d I_g + \left( 1 - \left( \frac{M_{cr}}{M_a} \right)^3 \right) I_{cr} < I_g$$

where

$M_{cr}$  = cracking moment

$M_a$  = moment at which the deflection is to be computed

$\beta_d$  = softening factor =  $0.5 \left[ \frac{E_p}{E_s} + 1 \right]$

$E_p$  = modulus of elasticity of the prestressing CFRP

$E_s$  = modulus of the elasticity of prestressing steel

$I_{cr}$  = cracking moment of inertia

The applicability of this equation was investigated by Kim<sup>21</sup> and Pirayeh Gar et al.<sup>22</sup> It was found that the equation proposed by ACI 440.4R-04<sup>19</sup> is sensitive to the ratio of the gross moment of inertia to the cracking moment of inertia  $I_g/I_{cr}$ . This expression, though empirical, provides a reasonable prediction for the CFRP prestressed concrete beams having an inertia ratio  $I_g/I_{cr}$  less than 25. The  $I_g/I_{cr}$  of composite prestressed concrete girders used in bridge construction is generally less than 25.

**Figure 13** presents a comparison of the experimental data with the analytical software predictions. As expected, the exclusion of the tension stiffening tends to overestimate the deflection behavior of the CFRP prestressed concrete beams. The prediction from the integrations of the curvature method used by the analysis software is on average within 7% (with tension stiffening using Bentz's 2000 model<sup>23</sup>) and 11% (without tension stiffening) of the experimental test results for the ultimate load and within 6% (with tension stiffening) and 4% (without tension stiffening) for the ultimate deflection. Similarly, the ACI 440.4R-04 effective moment of inertia method is within 11% of the experimental test results for the ultimate load and within 15% for the ultimate deflection.

## Deformability

**Table 4** presents a comparison of the deformability of the beams tested in this study using different approaches. According to the deformability index proposed by Abdelrahman,<sup>5</sup> the prestressed concrete beam using steel prestressing strands has 34% and 76% more deformability, respectively, than the beams prestressed with CFRP cable and CFRP bar. According to the deformability index proposed by Zou,<sup>12</sup> the prestressed concrete beam with steel strands exhibited 27% less deformability than the beams prestressed with CFRP cables and about equal deformability to the beam prestressed with CFRP bars. Similarly, using the deformability index defined in CAN/CSA-S6-06,<sup>24</sup> the prestressed concrete beam using steel prestressing strands showed 2.0 and 4.1 times more deformability, respectively, than the beams prestressed with CFRP cable and CFRP bar; however, an observation of the load-deflection response of the beams leads to the conclusion that these indices are insensitive to the actual load-deflection behavior. Therefore, a simplified approach defined in ACI 440.4R-04,<sup>19</sup> where the deformability index is the ratio of deflection of the beam at the ultimate moment to the ratio of deflection of the

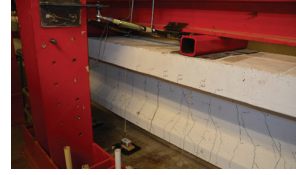
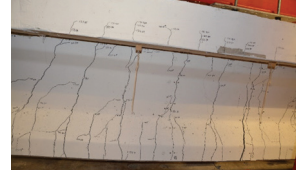
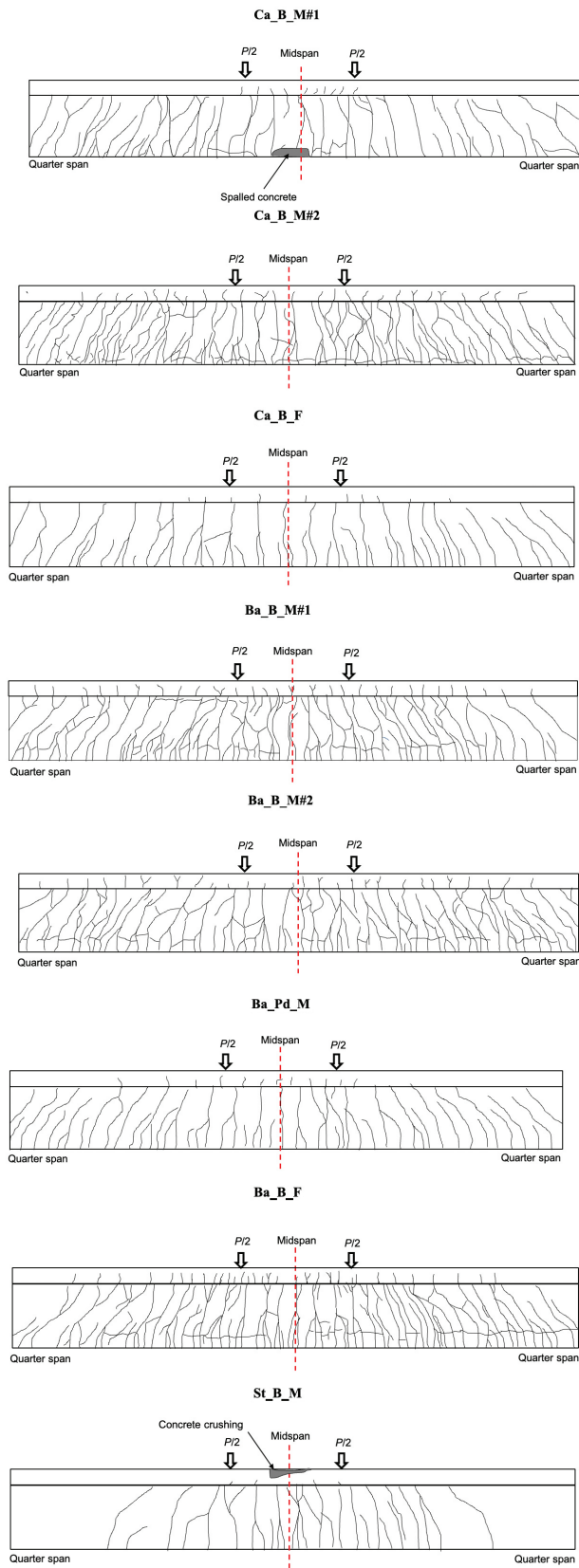


**Figure 12.** Crack distribution and failure mode of test beams at ultimate load. Note:  $P$  = applied load. 1 in. = 25.4 mm.

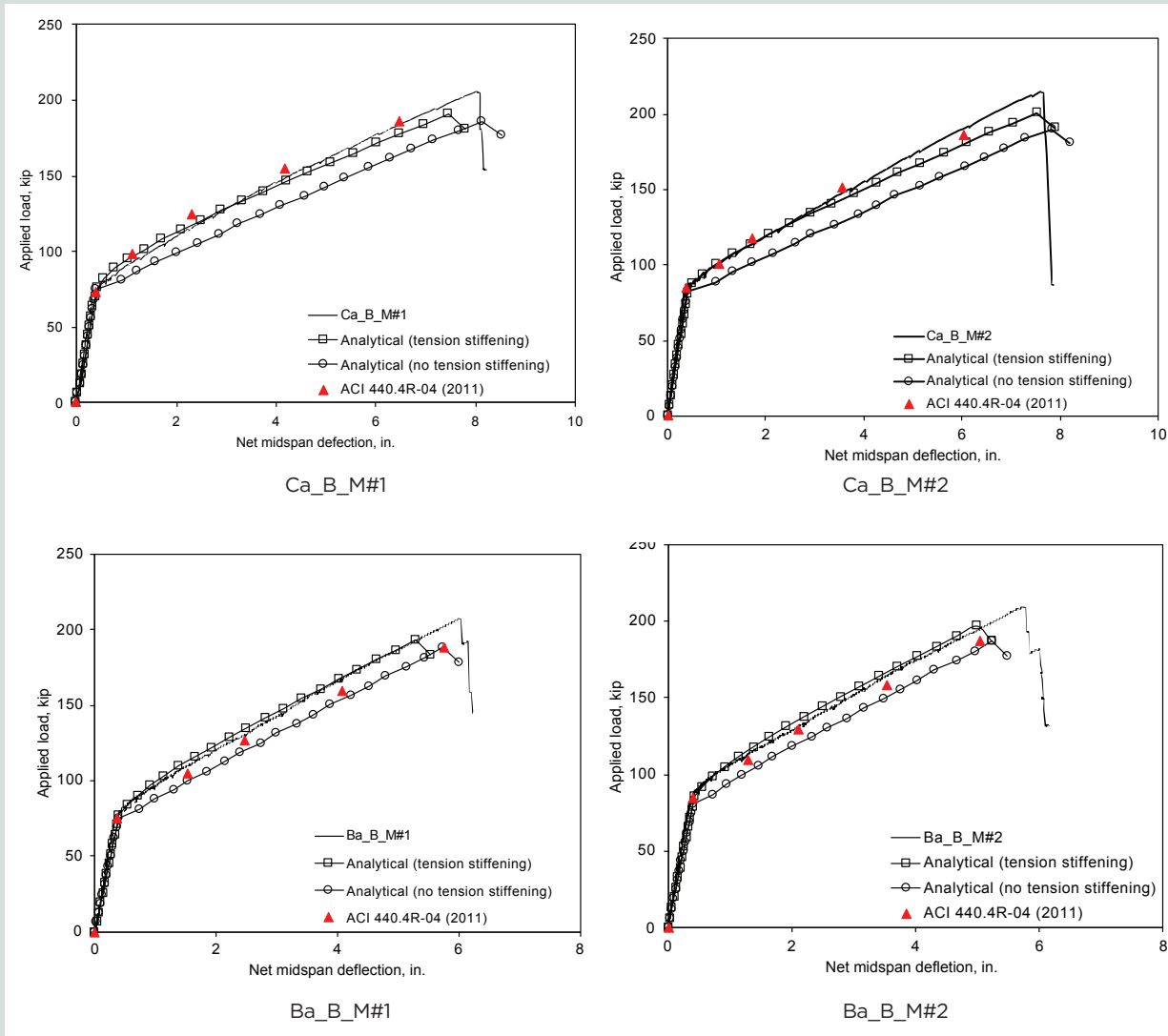


**Figure 13.** Experimental load-deflection values compared with the analytical prediction for the carbon-fiber-reinforced polymer prestressed concrete beams. Note: 1 in. = 25.4 mm; 1 kip = 4.448 kN.

beam at the cracking moment, is adopted here to quantify the deformability of the CFRP prestressed concrete beams. This definition can also be extended to the ratio of curvature at the ultimate moment to the curvature at the cracking moment. Accordingly, the deformability index  $DI$  of the CFRP prestressed concrete beams can be calculated as follows:

$$DI = \frac{\Delta_u}{\Delta_{cr}}$$

where

$\Delta_u$  = deflection at ultimate moment

$\Delta_{cr}$  = deflection at the cracking moment  $M_{cr}$

Table 4 summarizes the deformability indices of the beam. The deformability values indicate that this ratio  $DI$  is more representative of the load-deflection response of the beams investigated in this research.

## Conclusion

A total of eight prestressed concrete beams (three with prestressing CFRP cables, four with prestressing CFRP bars, and one with prestressing steel) were fabricated and tested under two flexural loading conditions: monotonic flexure and flexural fatigue. The following conclusions are made from the findings of this study:

- CFRP prestressed concrete beams demonstrated a higher strength (1.5 times the capacity for the same number of prestressing elements) and similar or lower deformability compared with steel prestressed concrete beams. The wide distribution of cracks and large deformation at failure for CFRP prestressed concrete beams indicates that CFRP prestressed concrete beams provide enough warning before failure.
- The beams prestressed with prestressing CFRP cables

**Table 4.** Deformability indices of the prestressed concrete beams

Beam identification	Deformability index				Failure mode
	Abdelrahman (1995)	Zou (2003)	CAN/CSA-S6-06 (2019)	ACI 440.4R-04 (2011)	
Ca_B_M#1	8.4	67	3.6	24	Cable rupture
Ca_B_M#2	8.1	51	2.2	21	
Ca_B_F	8.21	53	2.4	22	
Ba_B_M#1	6.41	43	1.8	16	
Ba_B_M#2	6.42	37	1.7	15	
Ba_B_F	6.23	46	1.7	17	
Ba_Pd_M	6.36	38	1.6	14	
St_B_M	11.3	37	7.5	21	Concrete crushing

exhibited larger crack widths, 1.3 to 1.7 times larger compared with the beams prestressed with CFRP bars. In addition, both beams pretensioned with prestressing CFRP cables and bars developed a large number of cracks before failure, similar to the beam pretensioned with steel strands.

- Negligible degradation in stiffness or strength was observed up to 2.3 million load cycles in CFRP prestressed concrete beams, indicating excellent fatigue performance for the induced stress range.
- The deformability equation based on the ratio of deflections at ultimate moment and cracking moment was found to be a reliable indicator of the flexural performance of CFRP prestressed concrete beams.
- Installing an anchorage system for both cables and bars is a tedious procedure that requires trained personnel. The size of the couplers controls the spacing and length of the prestressing elements.
- Both prestressing CFRP cable and bar anchorage systems showed acceptable performance in transferring loads, including transferring loads from steel strands to CFRP elements (using a coupler or transfer box) and anchor to CFRP prestressing element (using a wedge and sleeve) with no damage to the prestressing CFRP.
- A flexural design procedure based on the conditions of equilibrium and strain compatibility predicted the capacity of the CFRP prestressed concrete beams within 10% of the ultimate capacity from the experimental testing.
- The effective moment of inertia calculated according to ACI 4404R-04<sup>18</sup> used in deflection estimates provided a reasonable prediction (within 15%) up to the ultimate load.

## Acknowledgment

This research project was funded by the National Cooperative Highway Research Program (NCHRP) under project NCHRP 12-97. The views expressed in this paper are those of the authors and do not necessarily reflect the views of the funding agency.

## References

1. AASHTO. "AASHTO Innovation Initiative: Fast Fact Sheets." Accessed February 25, 2022. <http://aii.transportation.org/Pages/Carbon-Fiber-Reinforced-Polymer-Strands.aspx>.
2. Myers, J. J., and T. Viswanath. 2006. "A Worldwide Survey of Environmental Reduction Factors for Fiber Reinforced Polymers (FRP)." In *Structures Congress 2006: Structural Engineering and Public Safety Proceedings, May 18–21, 2006, St. Louis, MO*. Reston, VA: American Society of Civil Engineers.
3. Benmokrane, B., A. H. Ali, H. M. Mohamed, M. Robert, and A. ElSafty. 2015. "Durability Performance and Service Life of CFCC Tendons Exposed to Elevated Temperature and Alkaline Environment." *Journal of Composites for Construction* 20 (1). [https://doi.org/10.1061/\(ASCE\)CC.1943-5614.0000606](https://doi.org/10.1061/(ASCE)CC.1943-5614.0000606).
4. National Academies of Sciences, Engineering, and Medicine. 2019. *Design of Concrete Bridge Beams Prestressed with CFRP Systems*. Washington, DC: The National Academies Press. <https://doi.org/10.17226/25582>.
5. Abdelrahman, A. A. 1995. "Serviceability of Concrete Beams Prestressed by Fiber Reinforced Plastic Tendons." PhD diss., University of Manitoba, Winnipeg, MB, Canada.

6. Forouzannia, F., B. Gencturk, M. Dawood, and A. Belarbi. 2015. "Calibration of Flexural Resistance Factors for Load and Resistance Factor Design of Concrete Bridge Girders Prestressed with Carbon Fiber-Reinforced Polymers." *Journal of Composites for Construction* 20 (2). [https://doi.org/10.1061/\(ASCE\)CC.1943-5614.0000613](https://doi.org/10.1061/(ASCE)CC.1943-5614.0000613).
7. Naaman, A. E., K. H. Tan, S. M. Jeong, and F. M. Alkhaiiri. 1993. "Partially Prestressed Beams with Carbon Fiber Composite Strands: Preliminary Tests Evaluation." In *Fiber-Reinforced-Plastic Reinforcement for Concrete Structures—International Symposium*, ACI SP-38, pp. 441–464. Farmington Hills, MI: ACI (American Concrete Institute).
8. Grace, N. F., and S. B. Singh. 2003. "Design Approach for Carbon Fiber-Reinforced Polymer Prestressed Concrete Bridge Beams." *ACI Structural Journal* 100 (3): 365–376. <http://dx.doi.org/10.14359/12612>.
9. Grace, N., E. Jensen, V. Matsagar, and P. Penjendra. 2013. "Performance of an AASHTO Beam Bridge Prestressed with CFRP Tendons." *Journal of Bridge Engineering* 18 (2): 110–121. [https://doi.org/10.1061/\(ASCE\)BE.1943-5592.0000339](https://doi.org/10.1061/(ASCE)BE.1943-5592.0000339).
10. Naaman, A. E., and S. M. Jeong. 1995. "Structural Ductility of Concrete Beams Prestressed with FRP Tendons." In *Non-Metallic (FRP) Reinforcement for Concrete Structures: Proceedings of Second International RILEM Symposium*, L. Taerwe, ed., pp. 379–386. London, UK: Taylor & Francis. <https://doi.org/10.1201/9781482271621>.
11. Grace, N. F., and G. Abdel-Sayed. 1998. "Behavior of Externally Draped CFRP Tendons in Prestressed Concrete Bridges." *PCI Journal* 43 (5): 88–101. <https://doi.org/10.15554/pcij.09011998.88.101>.
12. Zou, P. X. 2003. "Flexural Behavior and Deformability of Fiber Reinforced Polymer Prestressed Concrete Beams." *Journal of Composites for Construction* 7 (4): 275–284. [https://doi.org/10.1061/\(ASCE\)1090-0268\(2003\)7:4\(275\)](https://doi.org/10.1061/(ASCE)1090-0268(2003)7:4(275)).
13. ASTM International. 2011. *Standard Test Method for Tensile Properties of Fiber Reinforced Polymer Matrix Composite Bars*. ASTM D7205/D7205M-06. West Conshohocken, PA: ASTM International. [https://doi.org/10.1520/D7205\\_D7205M-06](https://doi.org/10.1520/D7205_D7205M-06).
14. ASTM International. 2020. *Standard Test Method for Compressive Strength of Cylindrical Concrete Specimens*. ASTM C39/C39M-05. West Conshohocken, PA: ASTM International. [https://doi.org/10.1520/C0039\\_C0039M-05](https://doi.org/10.1520/C0039_C0039M-05).
15. AASHTO (American Association of State Highway and Transportation Officials). 2017. *AASHTO LRFD Bridge Design Specifications*. 8th ed. Washington, DC: AASHTO.
16. Erki, M. A., and S. H. Rizkalla. 1993. "Anchorages for FRP Reinforcement." *Concrete International* 15 (6): 54–59.
17. Sayed-Ahmed, E. Y., and N. G. Shrive. 1998. "A New Steel Anchorage System for Post-tensioning Applications Using Carbon Fibre Reinforced Plastic Tendons." *Canadian Journal of Civil Engineering* 25 (1): 113–127. <https://doi.org/10.1139/197-054>.
18. Collins, M. P., and D. Mitchell. 1997. *Prestressed Concrete Structures*. Toronto, ON, Canada: Response Publications.
19. ACI. 2011. *Prestressing Concrete Structures with FRP Tendons*. ACI 440.4R-04. Farmington Hills, MI: ACI.
20. Branson, D. E. 1965. "Instantaneous and Time-Dependent Deflections of Simple and Continuous Reinforced Concrete Beams." HPR report 7, part 1. Department of Civil Engineering and Auburn Research Foundation, Auburn University, Auburn, AL.
21. Kim, Y. J. 2010. "Flexural Response of Concrete Beams Prestressed with AFRP Tendons: Numerical Investigation." *Journal of Composites for Construction* 14 (6): 647–658. [https://doi.org/10.1061/\(ASCE\)CC.1943-5614.0000128](https://doi.org/10.1061/(ASCE)CC.1943-5614.0000128).
22. Pirayeh Gar, S., J. B. Mander, and S. Hurlbaeus. 2017. "Deflection of FRP Prestressed Concrete Beams." *Journal of Composites for Construction* 22 (2): 04017049. [https://doi.org/10.1061/\(ASCE\)CC.1943-5614.0000832](https://doi.org/10.1061/(ASCE)CC.1943-5614.0000832).
23. Bentz, E. C. 2000. "Sectional Analysis of Reinforced Concrete Members." PhD diss., University of Toronto, Toronto, ON, Canada.
24. CSA Group. 2019. *Canadian Highway Bridge Design Code*. CAN/CSA-S6-06. Toronto, ON, Canada: CSA Group.
25. AASHTO. "AASHTO Innovation Initiative: Fast Fact Sheets." Accessed February 25, 2022. <http://aii.transportation.org/Pages/Carbon-Fiber-Reinforced-Polymer-Strands.aspx>.

## Notation

- $E_p$  = modulus of elasticity of prestressing carbon-fiber-reinforced polymer
- $E_s$  = modulus of elasticity of prestressing steel
- $f'_c$  = concrete compressive strength



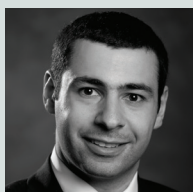
- $H$  = height of beam
- $I_{cr}$  = cracking moment of inertia
- $I_e$  = effective moment of inertia
- $I_g$  = gross moment of inertia
- $L$  = span length
- $M_a$  = moment at which deflection is to be computed
- $M_{cr}$  = cracking moment
- $P$  = applied load
- $\beta_d$  = softening factor
- $\Delta_{cr}$  = deflection at first cracking
- $\Delta_u$  = deflection at ultimate

## About the authors



Abdeldjelil Belarbi, PhD, PE, is the Hugh Roy and Lillie Crazz Cullen Distinguished Professor at the University of Houston in Texas. His primary research focuses on the constitutive modeling of structural concrete

and the use and design of advanced materials for new construction and strengthening of deteriorated civil engineering infrastructure.

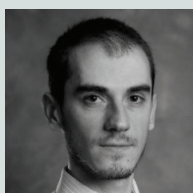


Mina Dawood, PhD, was an associate professor in the University of Houston in Texas during the course of this research. His research focused on the application of new and advanced materials, including carbon-fiber-reinforced

polymer, ultra-high-performance concrete, and shape memory alloy, in structural applications for both new construction and rehabilitation of existing structures.



Prakash Poudel, PhD, PE, is a Construction Technical Office PE at Ferrovia Construction US Corp in Houston. He received his bachelor's degree from Institute of Engineering, Nepal, and his PhD from the University of Houston.



Bora Gencturk, PhD, PE, is an associate professor in the Sonny Astani Department of Civil and Environmental Engineering at the University of Southern California, Los Angeles, California. He received his master's degrees and

his PhD from the University of Illinois at Urbana-Champaign.

## Abstract

Highway bridge beams are subjected to aggressive environments, temperature fluctuations, and millions of loading cycles throughout their service life. The combination of all of these effects can result in the reduction of the service life of structural components. In the past decades, more-durable composite materials, such as carbon-fiber-reinforced polymers (CFRPs) have been implemented in concrete structures to address problems

related to environmental durability. To date, prestressing applications of CFRP in beams have been mostly investigated for rectangular cross sections, which are not representative of the geometry used in modern highway bridges. In addition, the construction and detailing aspects of CFRP prestressed concrete beams have not been investigated outside of laboratory conditions. This paper describes an experimental investigation conducted on eight 40 ft (12 m) long AASHTO Type I prestressed concrete beams with 3 ft (0.9 m) wide composite concrete decks and detailed identically to highway bridge beams in practice. Three beams were pretensioned with carbon-fiber-composite cables, four beams with CFRP bars, and one with prestressing steel. The beams were tested under monotonic and fatigue loading. All CFRP prestressed concrete beams were designed to fail due to the rupture of the prestressing CFRP. The CFRP prestressed concrete beams exhibit several desirable features of the typical steel prestressed concrete beams in terms of serviceability and strength.

## Keywords

Carbon-fiber-reinforced polymer, CFRP, CFRP prestressed concrete beam, flexural behavior, prestressed concrete girder.

## Review policy

This paper was reviewed in accordance with the Precast/Prestressed Concrete Institute's peer-review process. The Precast/Prestressed Concrete Institute is not responsible for statements made by authors of papers in *PCI Journal*. No payment is offered.

## Publishing details

This paper appears in *PCI Journal* (ISSN 0887-9672) V. 67, No. 5, September–October 2022, and can be found at <https://doi.org/10.15554/pcij67.5-01>. *PCI Journal* is published bimonthly by the Precast/Prestressed Concrete Institute, 8770 W. Bryn Mawr Ave., Suite 1150, Chicago, IL 60631. Copyright © 2022, Precast/Prestressed Concrete Institute.

## Reader comments

Please address any reader comments to *PCI Journal* editor-in-chief Tom Klemens at [tklemens@pci.org](mailto:tklemens@pci.org) or Precast/Prestressed Concrete Institute, c/o *PCI Journal*, 8770 W. Bryn Mawr Ave., Suite 1150, Chicago, IL 60631. 